A.研究目的

神経難病であるPerry症候群における原因遺伝子dynactin の局在変化及び病的遺伝子変異によるミトコンドリア機能への影響を評価すること。

B.研究方法

本研究では主に培養細胞(HeLa 細胞)を用いた。以下にそれぞれの実験の詳細を述べる。

１．プラスミドDNA

Dynactin (p150glued)野生型にFLAGおよびEGFPをタグしたプラスミドDNAを作製し、Mutagenesis® (Stratagene 社製)を用いて、病因変異を挿入した変異型dynactin（G59S、G71A、G71E、G71V、T72P、Q74P）を作製した。

２．局在検討

HeLa 細胞に、Lipofectamine 2000®を用いて、dynactin 野生型・変異型を夫々強制発現し、24 時間後、48 時間後、72 時間後に各種抗体を用いて免疫細胞染色を行い、24 時間後に最もdynactin の発現が高いことを確認し，α-tubulin 抗体およびGFP 抗体で染色し，共焦点顕微鏡を用いて細胞内局在を検討した.

３．Lewy 小体における retromer 局在検討.

臨床的および病理学的にパーキンソン病の診断がついた3 症例の皮質および脳幹の組織切片を用いた. 抗体はSer129 リン酸化α-synuclein 抗体, M6PR 抗体，SNX-2 抗体を用いDAB 法で皮質型Lewy 小体および脳幹型Lewy 小体を染色し構成成分として局在するか検討した.

４．ミトコンドリア形態評価（電顕による）

HeLa 細胞に、Lipofectamine 2000® (Invitrogen 社製)を用いて、dynactin(p150glued)-GFP 野生型・変異型を夫々強制発現し、24 時間後にグルタールアルデヒドおよび酸化オスミウムにて固定し、電子顕微鏡にて評価した

５．ミトコンドリア膜電位評価

HeLa 細胞に、Lipofectamine 2000® (Invitrogen 社製)を用いて、dynactin(p150glued)-GFP 野生型・変異型を夫々強制発現し、24 時間後にMitoTracker-Red CMXRos 100nM に20 分間incubation し、GFP 陽性細胞におけるMitoTracker-Red CMXRos 蛍光強度をフローサイトメーター(FACSFortessa, BD Biosciences)を用いて評価した。

（倫理面への配慮）

剖検脳を用いて検討する事に関しては遺族に同意を得ており，順天堂大学倫理委員会の承認を受けて実施しており，倫理面に関する問題は無い.

C.研究結果

結果１： 正常型GFP-dynactin はα-tubulin と mergeしており，従来報告されているように軸索輸送に関わる機能が推定された．一方でG59S およびG71R 変異型dynactin は凝集体を形成する傾向にあった.

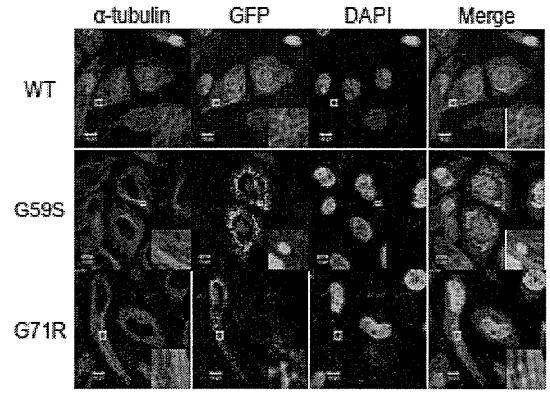

結果２：Retromer のマーカーであるSNX2 およびM6PR は皮質型Lewy 小体および脳幹型Lewy 小体のいずれにも局在しなかった.

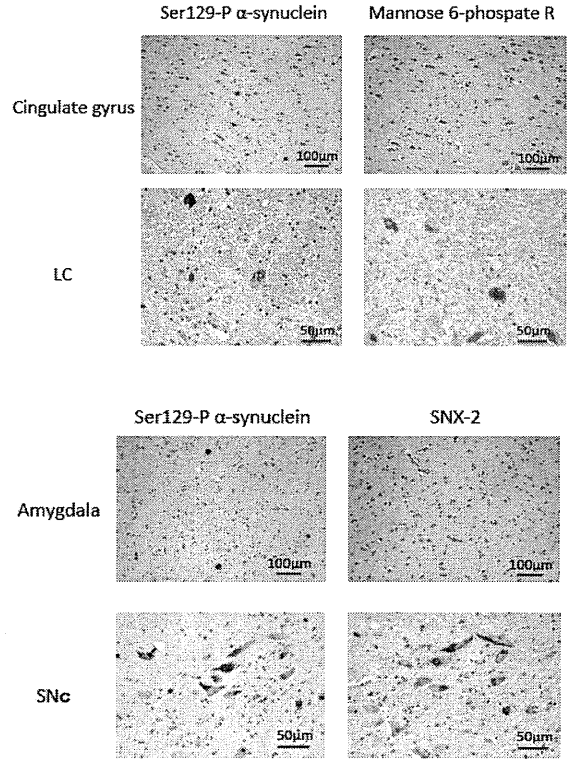

結果３： 野生型、変異型p150glued 強制発現細胞において、それぞれミトコンドリア形態を電子顕微鏡にて比較した。下図のように、コントロールベクター又は野生型強制発現細胞では、ミトコンドリアのクリステは保たれ、大きさに変化を認めなかった。しかし変異型強制発現細胞では、内部構造が破壊され、膨化したミトコンドリアが核周囲を中心に認められた（矢印)。

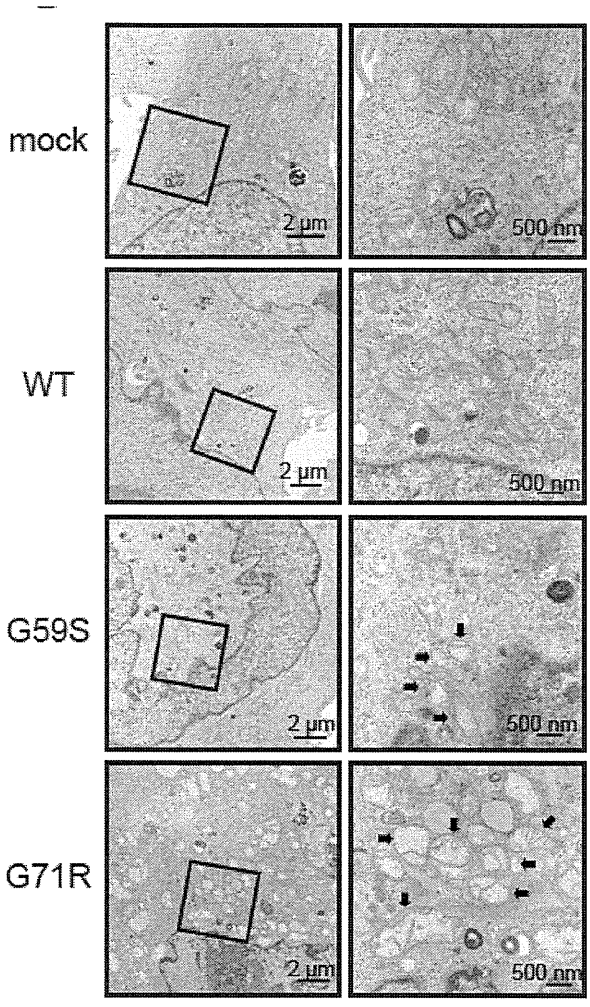

結果４：　変異型 p150glued の強制発現により、右図のように、Mitotracker-Red CMXRos の蛍光強度が減少した変異型導入細胞が著明に増加した。同現象は、GFP-p150glued 陽性細胞のみで評価した。

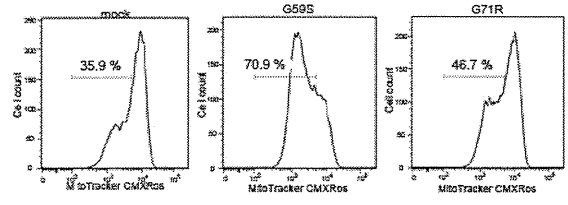

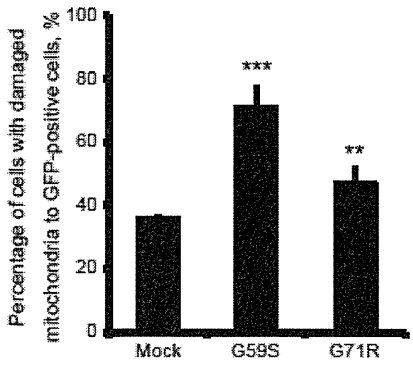

D.考察

G59S, G71R 変異型 dynactin の過剰発現は細胞質内凝集物を形成する．つまり dynactin の異常により retrograde の膜輸送が障害されることが示唆され，Lewy 小体をはじめとした神経変性疾患における凝集体形成に関係することが示唆された．しかし，SNX-2 および M6PR が Lewy 小体に含まれることはなく，retromer が Lewy 小体に含有される可能性は低いと考えられた．さらに，病的変異型 dynactin による細胞質内凝集物の形成とミトコンドリア機能との関連について検討を行ったが、MitoTracker-Red CMXRos の取り込みが低下（膜電位が低下していることを示す）し、かつ異常ミトコンドリアが凝集することから、機能を喪失したミトコンドリアにより引き起こされると判断した。分担研究者斉木の結果と併せて考察し、この異常ミトコンドリア凝集が内因性アポトーシス経路の原因になっていると推察された。

E.結論

病的変異型 dynactin は局在を変化させ神経細胞死を引き起こす可能性がある．また，凝集体を形成し異常ミトコンドリアの蓄積が関与している可能性がある．

F. 健康危険情報

特記事項なし

G.研究発表

1.論文発表

1. Sekigawa A, Fujita M, Sekiyama K, Takamatsu Y, Hatano T, Rockenstein E, La Spada AR, Masliah E, Hashimoto M. Distinct mechanisms of axonal globule foremation in mice expressing human wild type A-synuclein or dementia with Lewy bodies-linked P123H B-synuclein. Mol Brain. 2012; 5: 34. Doi: 10.1186/1756-6606-5-34.

2. Ujiie S, Hatano T, Kubo S, Imai S, Sato S, Uchihara T, Yagishita S, Hasegawa K, Kowa H, Sakai F, Hattori N. LRRK2 I2020T mutation is associated with tau pathology. Parkinsonism Relat Disord. 2012;7:819-23.

3. Usami Y, Hatano T, Imai S, Kubo S, Sato S, Saiki S, Fujioka Y, Ohba Y, Sato F, Funayama M, Eguchi H, Shiba K, Ariga H, Shen J, Hattori N. DJ-1 associates with synaptic membranes. Neurobiol Dis. 2011 Sep;43(3):651-62.

2.学会発表

1.「膜輸送の障害はLewy小体形成に関与するか」
波田野　琢, 久保　紳一郎, 高梨　雅史, 王子　悠, 森　聡生, 板谷　昌子, 服部　信孝
第52回日本神経学会（東京国際フォーラム）　平成24年5月22-25日

2. DJ-1の細胞内局在検討 宇佐見 由紀子, 波田野琢, 久保　紳一郎, 斉木　臣二, 佐藤　栄人, 大場　雄介, 有賀　寛芳, 服部　信孝
第52回日本神経学会（名古屋）　平成23年5月18-20日

H.知的所有権の取得状況（予定を含む）

1.特許取得：なし
2.実用新案登録：なし
3.その他：特になし

研究成果の刊行に関する一覧表

研究成果の刊行に関する一覧表（服部　信孝）

雑誌

発表者氏名	論文タイトル名	発表誌名	巻号	ページ	出版年
Tomiyama H, Yoshino H, Ogaki K, Li L, Yamashita C, Li Y, Funayama M, Sasaki R, Kokubo Y, Kuzuhara S, Hattori N.	PLA2G6 variant in Parkinson's disease.	J Hum Genet.	56	401-3	2011
Amo T, Sato S, Saiki S, Wolf AM, Toyomizu M, Gautier CA, Shen J, Ohta S, Hattori N.	Mitochondrial membrane potential decrease caused by loss of PINK1 is not due to proton leak, but to respiratory chain defects.	Neurobiol Dis.	41	111-8	2011
Usami Y, Hatano T, Imai S, Kubo S, Sato S, Saiki S, Fujioka Y, Ohba Y, Sato F, Funayama M, Eguchi H, Shiba K, Ariga H, Shen J, Hattori N.	DJ-1 associates with synaptic membranes.	Neurobiol Dis.	43	651-62	2011
Sato S, Hattori N.	Genetic mutations and mitochondrial toxins shed new light on the pathogenesis of Parkinson's disease.	Parkinsons Dis.	2011	ID:979231 (7 pages)	2011
Ogaki K, Li Y, Atsuta N, Tomiyama H, Funayama M, Watanabe H, Nakamura R, Yoshino H, Yato S, Tamura A, Naito Y, Taniguchi A, Fujita K, Izumi Y, Kaji R, Hattori N, Sobue G; Japanese Consortium for Amyotrophic Lateral Sclerosis research (JaCALS).	Analysis of C9orf72 repeat expansion in 563 Japanese patients with amyotrophic lateral sclerosis.	Neurobiol Aging	33	2527.e11-6	2012
Ogaki K, Li Y, Takanashi M, Ishikawa K, Kobayashi T, Nonaka T, Hasegawa M, Kishi M, Yoshino H, Funayama M, Tsukamoto T, Shioya K, Yokochi M, Imai H, Sasaki R, Kokubo Y, Kuzuhara S, Tomiyama H, Hattori N.	Analyses of the *MAPT*, *PGRN,* and *C9orf72* mutations in Japanese patients with FTLD, PSP, and CBS.	Parkinsonism Relat Disord	19	15-20	2013
Ando M, Funayama M, Li Y, Kashihara K, Murakami Y, Ishizu N, Toyoda C, Noguchi K, Hashimoto T, Nakano N, Sasaki R, Kokubo Y, Kuzuhara S, Ogaki K, Yamashita C, Yoshino H, Hatano T, Tomiyama H, Hattori N.	*VPS35* mutation in Japanese patients with typical Parkinson disease.	Mov Disord	27	1413-7	2012
Ujiie S, Hatano T, Kubo S, Imai S, Sato S, Uchihara T, Yagishita S, Hasegawa K, Kowa H, Sakai F, Hattori N.	LRRK2 I2020T mutation is associated with tau pathology.	Parkinsonism Relat Disord.	18	819-23	2012
Shiba-Fukushima K, Imai Y, Yoshida S, Ishihama Y, Kanao T, Sato S, Hattori N.	PINK1-mediated phosphorylation of the Parkin ubiquitin-like domain primes mitochondrial translocation of Parkin and regulates mitophagy.	Sci Rep.	2	1002	2012

研究成果の刊行に関する一覧表（坪井　義夫）

書籍

著者氏名	論文タイトル名	書籍全体の編集者名	書　籍　名	出版社名	出版地	出版年	ページ
坪井義夫	Perry 症候群. －始まりは一人の患者から－		Medical Science Digest (MSD)	ニューサイエンス社	東京	2012	38(2): 2-4(48-50)

研究成果の刊行に関する一覧表（佐藤　栄人）

雑誌

発表者氏名	論文タイトル名	発表誌名	巻号	ページ	出版年
Usami Y, Hatano T, Imai S, Kubo S, Sato S, Saiki S, Fujioka Y, Ohba Y, Sato F, Funayama M, Eguchi H, Shiba K, Ariga H, Shen J, Hattori N.	DJ-1 associates with synaptic membranes.	Neurobiol Dis.	43	651-62	2011
Sato S, Hattori N.	Genetic mutations and mitochondrial toxins shed new light on the pathogenesis of Parkinson's disease.	Parkinsons Dis.	2011	ID: 979231	2011
Amo T, Sato S, Saiki S, Wolf AM, Toyomizu M, Gautier CA, Shen J, Ohta S, Hattori N.	Mitochondrial membrane potential decrease caused by loss of PINK1 is not due to proton leak, but to respiratory chain defects.	Neurobiol Dis.	41	111-8	2011
Ujiie S, Hatano T, Kubo S, Imai S, Sato S, Uchihara T, Yagishita S, Hasegawa K, Kowa H, Sakai F, Hattori N.	LRRK2 I2020T mutation is associated with tau pathology.	Parkinsonism Relat Disord.	18	819-23	2012
Shiba-Fukushima K, Imai Y, Yoshida S, Ishihama Y, Kanao T, Sato S, Hattori N.	PINK1-mediated phosphorylation of the Parkin ubiquitin-like domain primes mitochondrial translocation of Parkin and regulates mitophagy.	Sci Rep.	2	1002	2012

研究成果の刊行に関する一覧表（富山　弘幸）

書籍

著者氏名	論文タイトル名	書籍全体の編集者名	書　籍　名	出版社名	出版地	出版年	ページ
舩山学、富山弘幸	パーキンソン病の基礎研究最前線：実地医家のための minimum requirement		Modern Physician	新興医学出版社	東京	2012	32(2): 201-5
富山弘幸	Perry症候群とDCTN1遺伝子異常		Medical Science Digest (MSD)	ニューサイエンス社	東京	2012	38(4): 2-4(138-140)
富山弘幸.	パーキンソン病の発症に遺伝子の関与はあるのか？：　あなたも名医！パーキンソン病Q&A　version 2.	服部信孝	日本医事新報 jmed mook 第23号	日本医事新報社	東京	2012	17-24.

雑誌

発表者氏名	論文タイトル名	発表誌名	巻号	ページ	出版年
Tomiyama H, Yoshino H, Ogaki K, Li L, Yamashita C, Li Y, Funayama M, Sasaki R, Kokubo Y, Kuzuhara S, Hattori N.	PLA2G6 variant in Parkinson's disease.	J Hum Genet.	56	401-3	2011
Ogaki K, Li Y, Atsuta N, Tomiyama H, Funayama M, Watanabe H, Nakamura R, Yoshino H, Yato S, Tamura A, Naito Y, Taniguchi A, Fujita K, Izumi Y, Kaji R, Hattori N, Sobue G; Japanese Consortium for Amyotrophic Lateral Sclerosis research (JaCALS).	Analysis of C9orf72 repeat expansion in 563 Japanese patients with amyotrophic lateral sclerosis.	Neurobiol Aging	33	2527.e11-6	2012
Ogaki K, Li Y, Takanashi M, Ishikawa K, Kobayashi T, Nonaka T, Hasegawa M, Kishi M, Yoshino H, Funayama M, Tsukamoto T, Shioya K, Yokochi M, Imai H, Sasaki R, Kokubo Y, Kuzuhara S, Tomiyama H, Hattori N.	Analyses of the *MAPT*, *PGRN*, and *C9orf72* mutations in Japanese patients with FTLD, PSP, and CBS.	Parkinsonism Relat Disord	19	15-20	2013
Ando M, Funayama M, Li Y, Kashihara K, Murakami Y, Ishizu N, Toyoda C, Noguchi K, Hashimoto T, Nakano N, Sasaki R, Kokubo Y, Kuzuhara S, Ogaki K, Yamashita C, Yoshino H, Hatano T, Tomiyama H, Hattori N.	*VPS35* mutation in Japanese patients with typical Parkinson disease.	Mov Disord	27	1413-7	2012

研究成果の刊行に関する一覧表（斉木　臣二）

雑誌

発表者氏名	論文タイトル名	発表誌名	巻号	ページ	出版年
Saiki S, Sasazawa Y, Imamichi Y, Kawajiri S, Fujimaki T, Tanida I, Kobayashi H, Sato F, Kei-Ichi Ishikawa, Sato S, Imoto M, Hattori N.	Caffeine induces apoptosis by enhancement of autophagy via PI3K/Akt/mTOR/p70S6K inhibition.	Autophagy	7	176-87	2011
Kawajiri S, Machida Y, Saiki S, Sato S, Hattori N.	Zonisamide reduces cell death in SH-SY5Y cells via an anti-apoptotic effect and by upregulating MnSOD.	Neurosci Lett	481	88-91	2010

研究成果の刊行に関する一覧表（波田野　琢）

雑誌

発表者氏名	論文タイトル名	発表誌名	巻号	ページ	出版年
Usami Y, Hatano T, Imai S, Kubo S, Sato S, Saiki S, Fujioka Y, Ohba Y, Sato F, Funayama M, Eguchi H, Shiba K, Ariga H, Shen J, Hattori N.	DJ-1 associates with synaptic membranes.	Neurobiol Dis.	43	651-62	2011
Ujiie S, Hatano T, Kubo S, Imai S, Sato S, Uchihara T, Yagishita S, Hasegawa K, Kowa H, Sakai F, Hattori N.	LRRK2 I2020T mutation is associated with tau pathology.	Parkinsonism Relat Disord.	18	819-23	2012
Sekigawa A, Fujita M, Sekiyama K, Takamatsu Y, Hatano T, Rockenstein E, La Spada AR, Masliah E, Hashimoto M	Distinct mechanisms of axonal globule formation in mice expressing human wild type α-synuclein or dementia with Lewy bodies-linked P123H β-synuclein.	Mol Brain.	5	34 doi: 10.1186/1756-6606-5-34.	2012

研究成果の刊行物・別刷

Parkinsonism and Related Disorders 17 (2011) 493–494

Contents lists available at ScienceDirect

Parkinsonism and Related Disorders

journal homepage: www.elsevier.com/locate/parkreldis

Letter to the Editor

Analysis of *PLA2G6* in patients with frontotemporal type of dementia☆

Keywords:
Parkinson's disease
Parkinsonism
PARK14
PLA2G6
Frontotemporal lobar degeneration (FTLD)

To the Editor

To increase understanding of *PARK14*-linked parkinsonism and the roles of *PLA2G6*, we would like to report additional data related to our recent study "Phenotypic spectrum of patients with *PLA2G6* mutation and *PARK14*-linked parkinsonism" [1].

PLA2G6 is the causative gene for infantile neuroaxonal dystrophy (INAD), neurodegeneration associated with brain iron accumulation, and Karak syndrome [2,3]. Recently, Paisan-Ruiz *et al* reported that *PLA2G6* was the causative gene for autosomal recessive early-onset dystonia-parkinsonism (*PARK14*-linked parkinsonism) [4]. We have also found three patients (two families) with *PARK14*-linked parkinsonism [1]. Intriguingly, our two Japanese index patients (age/age at onset = 35/20 and 33/25 years old) and the previously reported two index patients all had dementia with frontal lobar dysfunction including: frontal executive dysfunction, frontal lobar atrophy, or frontal lobar hypoperfusion on neuroimaging [1,4].

In order, to determine the significance of the *PLA2G6* mutation, we conducted extended mutation analysis in 23 Japanese patients (male 12, female 11) with frontotemporal type dementia (suspected frontotemporal dementia based on clinical features, frontotemporal lobar atrophy on MRI/CT, or frontotemporal lobar hypoperfusion on SPECT). Among them, 11 patients had family histories of a frontotemporal type of dementia (5 autosomal dominant, 5 autosomal recessive mode of inheritance, 1 unknown familial dementia, 9 sporadic dementia, and 1 unknown family history). Age at sampling was 66.0 ± 13.4 (mean ± SD), range 40–85 year. Age at onset was 58.6 ± 11.7 (mean ± SD), range 38–78 year. This cohort had later age/age at onset than that of the previously reported *PLA2G6*-positive patients with frontotemporal type of dementia. The study was approved by the ethics committee of Juntendo University and each subject provided written informed consent.

Direct sequencing of all the *PLA2G6* exons revealed no pathogenic mutations or significant SNPs. Thus, although all our patients with *PLA2G6* mutations had dementia with frontotemporal lobar atrophy, our additional data indicate that *PLA2G6* mutation may not play a major role in general frontotemporal type of dementia at least in the Japanese population including the heterozygous mutation.

Taken together with the previous reports, our data suggest that *PLA2G6* mutations should be considered more likely in patients with early-onset frontotemporal type of dementia than in patients with later-onset frontotemporal type of dementia. The etiology of the majority of frontotemporal lobar degeneration is still unknown except for some cases with *MAPT* or *PGRN* mutations. Therefore, the etiology of the frontotemporal lobar degeneration should be clarified by clinicogenetic studies or other approaches.

Disclosure

This study was supported by a grant from the Japanese Ministry of Education, Culture, Sports, Science and Technology, Grants-in-Aid for Scientific Research (to HT: 21591098 and to NH: 090052131), for Scientific Research on Priority Areas (to NH: 08071510) and Health and Labour Sciences Research Grants from the Japanese Ministry of Health, Labour and Welfare (to NH: H19-021 and H20-015). This work was partially supported by Grants-in-Aid from the Research Committee of CNS Degenerative Diseases and Perry syndrome, the Ministry of Health, Labour and Welfare of Japan (to NH and HT: 22140901).

References

[1] Yoshino H, Tomiyama H, Tachibana N, Ogaki K, Li Y, Funayama M, et al. Phenotypic spectrum of patients with *PLA2G6* mutation and *PARK14*-linked parkinsonism. Neurology 2010;75:1356–61.
[2] Morgan NV, Westaway SK, Morton JE, Gregory A, Gissen P, Sonek S, et al. PLA2G6 encoding a phospholipase A2, is mutated in neurodegenerative disorders with high brain iron. Nat Genet 2006;38:752–4.
[3] Mubaidin A, Roberts E, Hampshire D, Dehyyat M, Shurbaji A, Mubaidien M, et al. Karak syndrome: a novel degenerative disorder of the basal ganglia and cerebellum. J Med Genet 2003;40:543–6.
[4] Paisan-Ruiz C, Bhatia KP, Li A, Hernandez D, Davis M, Wood NW, et al. Characterization of PLA2G6 as a locus for dystonia-parkinsonism. Ann Neurol 2009; 65:19–23.

Hiroyuki Tomiyama*
Department of Neurology, Juntendo University School of Medicine, 2-1-1 Hongo, Bunkyo-ku, Tokyo 113-8421, Japan
* Corresponding author. Tel.: +81 3 5802 1073; fax: +81 3 5800 0547.
E-mail address: tomiyama@juntendo.ac.jp

Hiroyo Yoshino
Research Institute for Diseases of Old Age, Juntendo University School of Medicine, Tokyo, Japan

☆ The review of this paper was entirely handled by an Associate Editor, Eng-King Tan.

1353-8020/$ – see front matter
doi:10.1016/j.parkreldis.2011.03.011

Nobutaka Hattori
Department of Neurology, Juntendo University School of Medicine, 2-1-1 Hongo, Bunkyo-ku, Tokyo 113-8421, Japan

Research Institute for Diseases of Old Age, Juntendo University School of Medicine, Tokyo, Japan

5 March 2011

YNBDI-02241; No. of pages: 8; 4C:

Neurobiology of Disease xxx (2010) xxx–xxx

Contents lists available at ScienceDirect

Neurobiology of Disease

journal homepage: www.elsevier.com/locate/ynbdi

Mitochondrial membrane potential decrease caused by loss of PINK1 is not due to proton leak, but to respiratory chain defects

Taku Amo [a,1], Shigeto Sato [b], Shinji Saiki [b], Alexander M. Wolf [a], Masaaki Toyomizu [c], Clement A. Gautier [d], Jie Shen [d], Shigeo Ohta [a], Nobutaka Hattori [b,*]

[a] Department of Biochemistry and Cell Biology, Institute of Development and Aging Sciences, Graduate School of Medicine, Nippon Medical School, 1-396 Kosugi-cho, Nakahara-ku, Kawasaki 211-8533, Japan
[b] Department of Neurology, Juntendo University School of Medicine, 2-1-1 Hongo, Bunkyo-ku, Tokyo 113-8421, Japan
[c] Animal Nutrition, Life Sciences, Graduate School of Agricultural Science, Tohoku University, 1-1 Tsutsumidori-Amamiyamachi, Aoba-ku, Sendai 981-8555, Japan
[d] Center for Neurologic Diseases, Brigham and Women's Hospital, Program in Neuroscience, Harvard Medical School, Boston, MA 02115, USA

ARTICLE INFO

Article history:
Received 29 June 2010
Revised 17 August 2010
Accepted 25 August 2010
Available online xxxx

Keywords:
Parkinson's disease
Mitochondria
PINK1
Parkin
Membrane potential
Oxidative phosphorylation
Modular kinetic analysis
Proton leak
Reactive oxygen species

ABSTRACT

Mutations in *PTEN-induced putative kinase 1* (*PINK1*) cause a recessive form of Parkinson's disease (PD). PINK1 is associated with mitochondrial quality control and its partial knock-down induces mitochondrial dysfunction including decreased membrane potential and increased vulnerability against mitochondrial toxins, but the exact function of PINK1 in mitochondria has not been investigated using cells with null expression of PINK1. Here, we show that loss of PINK1 caused mitochondrial dysfunction. In PINK1-deficient ($PINK1^{-/-}$) mouse embryonic fibroblasts (MEFs), mitochondrial membrane potential and cellular ATP levels were decreased compared with those in littermate wild-type MEFs. However, mitochondrial proton leak, which reduces membrane potential in the absence of ATP synthesis, was not altered by loss of PINK1. Instead, activity of the respiratory chain, which produces the membrane potential by oxidizing substrates using oxygen, declined. H_2O_2 production rate by $PINK1^{-/-}$ mitochondria was lower than $PINK1^{+/+}$ mitochondria as a consequence of decreased oxygen consumption rate, while the proportion (H_2O_2 production rate per oxygen consumption rate) was higher. These results suggest that mitochondrial dysfunctions in PD pathogenesis are caused not by proton leak, but by respiratory chain defects.

Introduction

Parkinson's disease (PD) is a neurodegenerative disease characterized by loss of dopaminergic neurons in the substantia nigra. Mitochondrial dysfunction has been proposed as a major factor in the pathogenesis of sporadic and familial PD (Abou-Sleiman et al., 2006). In particular, the identification of mutations in *PTEN-induced putative kinase 1* (*PINK1*) has strongly implicated mitochondrial dysfunction owing to its loss of function in the pathogenesis of PD (Valente et al., 2004). PINK1 contains an N-terminal mitochondrial targeting sequence (MTS) and a serine/threonine kinase domain (Valente et al., 2004). PINK1 kinase activity is crucial for mitochondrial maintenance via TRAP phosphorylation (Pridgeon et al., 2007). Loss of PINK1 function induces increased vulnerability to various stresses (Exner et al., 2007; Haque et al., 2008; Pridgeon et al., 2007; Wood-Kaczmar et al., 2008). However, silencing of PINK1 has only been partial and only one study has been performed to assess mitochondrial functions in steady and artificial states with complete ablation of PINK1 expression (Gautier et al., 2008).

Several studies have shown that PINK1 acts upstream of parkin in the same genetic pathway (Clark et al., 2006; Park et al., 2006) and co-overexpressed PINK1 and parkin both co-localized to mitochondria (Kim et al., 2008). Overexpression of PINK1 promotes mitochondrial fission (Yang et al., 2008). Fission followed by selective fusion segregates dysfunctional mitochondria and permits their removal by autophagy (Twig et al., 2008). PINK1 loss-of-function decreases mitochondrial membrane potential (Chu, 2010) and the PINK1–parkin pathway is associated with mitochondrial elimination in cultured cells treated with the mitochondrial uncoupler carbonyl cyanide *m*-chlorophenylhydrazone (CCCP), which causes mitochondrial depolarization (Geisler et al., 2010; Kawajiri et al., 2010; Matsuda et al., 2010; Narendra et al., 2008, 2010; Vives-Bauza et al., 2010). However, the exact mechanism underlying the mitochondrial depolarization induced by PINK1 defects leading to mitochondrial autophagy has not been examined in detail.

Abbreviations: $\Delta\psi$, mitochondrial membrane potential; FCCP, carbonyl cyanide *p*-trifluoromethoxyphenylhydrazone; MEFs, mouse embryonic fibroblasts; PD, Parkinson's disease; PINK1, PTEN-induced putative kinase 1; ROS, reactive oxygen species; TMRM, tetramethylrhodamine methyl ester; TPMP, triphenylmethylphosphonium.

* Corresponding author. Fax: +81 3 5800 0547.
E-mail address: nhattori@juntendo.ac.jp (N. Hattori).
[1] Present address: Department of Applied Chemistry, National Defense Academy, 1-10-20 Hashirimizu, Yokosuka 239-8686, Japan.

Available online on ScienceDirect (www.sciencedirect.com).

0969-9961/$ – see front matter © 2010 Elsevier Inc. All rights reserved.
doi:10.1016/j.nbd.2010.08.027

Here, we describe a detailed characterization of mitochondria in PINK1-deficient cells. We show that PINK1 deficiency causes a decrease in mitochondrial membrane potential, which is not due to proton leak, but to respiratory chain defects.

Materials and methods

PINK1 knock-out mouse embryonic fibroblasts (MEFs)

PINK1 knock-out MEFs were prepared and cultured as described previously (Matsuda et al., 2010). Mouse embryonic fibroblasts (MEFs) were derived from E12.5 embryos containing littermate 4 mice of each genotype. Embryos were mechanically dispersed by repeated passage through a P1000 pipette tip and plated with MEF media containing DME, 10% FCS, 1× nonessential amino acids, 1 mM L-glutamine, penicillin/streptomycin (invitrogen). The $\psi 2$ cell line, an ecotropic retrovirus packaging cell line, was maintained in Dulbecco's modified Eagle medium (DMEM, Sigma) with 5% fetal bovine serum and 50 μg/ml kanamicin. Transfection of the $\psi 2$ cells with pMESVTS plasmids containing an SV40 large T antigen was performed by lipofection method according to the manual provided by the manufacturer (GIBCO BRL). Five micrograms of the plasmids was used for each transfection. Transfectants were selected by G418 at the concentration of 0.5 mg/ml, and 10 clonal cell lines were established. The highest titer of 5×10^4 cfu/ml was obtained for the conditioned medium of a cell line designated $\psi 2$SVTS1. 10^6 MEFs were plated onto a 10-cm culture dish and kept at 33 °C for 48 hours. Then medium was replaced with 2 ml supplemented with polybrene-supplemented medium conditioned by the $\psi 2$SVTS1 cells at confluency for 3 days. Infection was continued for 3 hours, and the medium was replaced with a fresh one. The infected MEFs were cultured at 33 °C until immortalized cells were obtained.

We confirmed that the differences we detected in this study were due to the PINK1 deficiency, not to artificial effects by immortalization, by measuring cellular respiration rates of not immortalized MEFs from other littermates (Supplemental figure). The respiration rates of not immortalized MEFs were slightly slower than those of immortalized MEFs, but the differences between PINK1$^{+/+}$ and $^{-/-}$ MEFs were consistent (Fig. 2A).

Cell growth

Cells were seeded in 12-well plates at density of $3\sim6\times10^3$ cells/well and incubated in DMEM high glucose medium (4.5 g/l glucose and 1 mM sodium pyruvate) supplemented with 10% fetal bovine serum. After a day, the medium was replaced with DMEM glucose-free medium supplemented with 1 g/l galactose, 1 mM sodium pyruvate and 10% fetal bovine serum (DMEM galactose medium) at 37 °C in an incubator with a humidified atmosphere of 5% CO_2. Cells were trypsinized and live cells were assessed by trypan blue dye exclusion.

Mitochondrial morphological changes

Cells were seeded in 6-well plates at 2.0×10^5/well and incubated in DMEM high glucose medium (4.5 g/l glucose and 1 mM sodium pyruvate) supplemented with 10% fetal bovine serum and 1% penicillin/streptomycin. After a day, the medium was replaced with DMEM glucose-free medium supplemented with 1 g/l galactose, 1 mM sodium pyruvate and 10% fetal bovine serum (DMEM galactose medium) at 37 °C in an incubator with a humidified atmosphere of 5% CO_2. 24 hours later, cells were fixed and immunostained with anti-Tom20 antibody to visualize mitochondria according to a protocol as previously described (Kawajiri et al., 2010). All images were obtained using an Axioplan 2 imaging microscope (Carl Zeiss, Oberkochen, Germany).

Cellular ATP levels

Intracellular ATP levels were determined by a cellular ATP assay kit (TOYO B-Net, Tokyo, Japan) according to the manufacturer's instructions using a Lumat LB9507 luminometer (Berthold Technology, Bad Wildbad, Germany).

Membrane potential

Fluorescence images were recorded using a multi-dimensional imaging workstation (AS MDW, Leica Microsystems, Wetzlar, Germany) with a climate chamber maintained at 37 °C. Fluorescence was quantified with a CCD camera (CoolSnap HQ, Roper Scientific, Princeton, NJ) using a 20× objective. Cells were stained for 1 hour with a non-quenching concentration (20 nM) of tetramethylrhodamine methyl ester (TMRM) in a 96-well plate. The cell-permeable cationic dye TMRM accumulates in mitochondria according to the Nernst equation. Nuclei were stained with 250 nM Hoechst 34580. Mitochondrial TMRM fluorescence was integrated in a 40-μm diameter circular area around the nucleus, and the minimum fluorescence in this area was subtracted as background fluorescence.

Cell respiration

Cell respiration was measured at 37 °C using the Oxygen Meter Model 781 and the Mitocell MT200 closed respiratory chamber (Strathkelvin Instruments, North Lanarkshire, United Kingdom). Cells were cultured in DMEM with 4.5 g/l of glucose supplemented with 10% FBS. Cells were then trypsinized and resuspended in Leibovitz's L-15 medium (Invitrogen) at density of 8.0×10^6 cells/ml. The oxygen respiration rate was measured under each of the following three conditions: basal rate (no additions); State 4 (no ATP synthesis) [after addition of 1 μg/ml oligomycin (Sigma)], uncoupled [after addition of 3 μM FCCP (carbonyl cyanide *p*-trifluoromethoxyphenylhydrazone; Sigma)] using Strathkelvin 949 Oxygen System. After sequential measurements, the endogenous respiration rate was determined by adding 1 μM rotenone + 2 μM myxothiazol.

Mitochondrial respiration and membrane potential

Mitochondria were prepared from cultured MEFs as previously described (Amo and Brand, 2007). Mitochondrial oxygen consumption with 5 mM succinate as a respiratory substrate was measured at 37 °C using a Clark electrode (Rank Brothers, Cambridge, United Kingdom) calibrated with air-saturated respiration buffer comprising 0.115 M KCl, 10 mM KH_2PO_4, 3 mM HEPES (pH 7.2), 2 mM $MgCl_2$, 1 mM EGTA and 0.3% (w/v) defatted BSA, assumed to contain 406 nmol atomic oxygen/ml (Reynafarje et al., 1985). Mitochondrial membrane potential ($\Delta\psi$) was measured simultaneously with respiratory activity using an electrode sensitive to the lipophilic cation $TPMP^+$ (triphenylmethylphosphonium) (Brand, 1995). Mitochondria were incubated at 0.5 mg/ml in the presence of 80 ng/ml nigericin (to collapse the pH gradient so that the proton motive force was expressed exclusively as $\Delta\psi$) and 2 μM rotenone (to inhibit complex I). The $TPMP^+$-sensitive electrode was calibrated with sequential additions of $TPMP^+$ up to 2 μM, then 5 mM succinate was added to initiate respiration. Experiments were terminated with 2 μM FCCP, allowing correction for any small baseline drift. $\Delta\psi$ was calculated from the distribution of $TPMP^+$ across the mitochondrial inner membrane using a binding correction factor of 0.35 mg protein/μl. Respiratory rates with 4 mM pyruvate + 1 mM malate as a substrate in State 3 (with 0.25 mM ADP) and State 4 (with 1 μg/ml oligomycin) were determined using the Oxygen Meter Model 781 and the Mitocell MT200 closed respiratory chamber (Strathkelvin Instruments).

Please cite this article as: Amo, T., et al., Mitochondrial membrane potential decrease caused by loss of PINK1 is not due to proton leak, but to respiratory chain defects, Neurobiol. Dis. (2010), doi:10.1016/j.nbd.2010.08.027

Modular kinetic analysis

To investigate differences in oxidative phosphorylation caused by PINK1 knock-out, we applied a systems approach, namely modular kinetic analysis (Amo and Brand, 2007; Brand, 1990). This analyzes the kinetics of the whole of oxidative phosphorylation divided into three modules connected by their common substrate or product, $\Delta\psi$. The modules are (i) the reactions that produce $\Delta\psi$, consisting of the substrate translocases, dehydrogenases and other enzymes and the components of the respiratory chain, called 'substrate oxidation'; (ii) the reactions that consume $\Delta\psi$ and synthesize, export and dephosphorylate ATP, consisting of ATP synthase, the phosphate and adenine nucleotide translocases and any ATPases that may be present, called the 'phosphorylating system'; and (iii) the reactions that consume $\Delta\psi$ without ATP synthesis, called the 'proton leak' (Brand, 1990). The analysis reports changes anywhere within oxidative phosphorylation that are functionally important but is unresponsive to changes that have no functional consequences. Comparison of the kinetic responses of each of the three modules to $\Delta\psi$ obtained using mitochondria isolated from PINK1$^{+/+}$ and PINK1$^{-/-}$ MEFs would reveal any effects of PINK1 on the kinetics of oxidative phosphorylation. Oxygen consumption and $\Delta\psi$ were measured simultaneously using mitochondria incubated with 80 ng/ml nigericin and 4 μM rotenone. Respiration was initiated by 5 mM succinate. The kinetic behavior of a '$\Delta\psi$-producer' can be established by specific modulation of a $\Delta\psi$-consumer and the kinetics of a consumer can be established by specific modulation of a $\Delta\psi$-producer (Brand, 1998). To measure the kinetic response of proton leak to $\Delta\psi$, the State 4 (non-phosphorylating) respiration of mitochondria in the presence of oligomycin (0.8 μg/ml; to prevent any residual ATP synthesis), which was used solely to drive the proton leak, was titrated with malonate (up to 8 mM). In a similar way, State 4 respiration was titrated by FCCP (up to 1 μM) for measurement of the kinetic response of substrate oxidation to $\Delta\psi$. State 3 (maximal rate of ATP synthesis) was obtained by addition of excess ADP (1 mM). Titration of State 3 respiration with malonate (up to 1.1 mM) allowed measurement of the kinetics of the $\Delta\psi$-consumers (the sum of the phosphorylating system and proton leak). The coupling efficiencies of oxidative phosphorylation were calculated from the kinetic curves as the percentage of mitochondrial respiration rate at a given $\Delta\psi$ that was used for ATP synthesis and was therefore inhibited by oligomycin. Note that any slip reactions will appear as proton leak in this analysis (Brand et al., 1994).

Mitochondrial ROS production

Mitochondrial ROS production rate was assessed by measurement of H_2O_2 generation rate, determined fluorometrically by measurement of oxidation of Amplex Red to fluorescent resorufin coupled to the enzymatic reduction of H_2O_2 by horseradish peroxidase using a spectrofluorometer RF-5300PC (Shimadzu, Kyoto, Japan). The H_2O_2 generation rate was measured in non-phosphorylating conditions (=State 4) using either pyruvate/malate or succinate as respiratory substrates. Mitochondria were incubated at 0.1 mg/ml in respiration buffer. All incubations also contained 5 μM Amplex Red, 2 U/ml horseradish peroxidase and 8 U/ml superoxide dismutase. The reaction was initiated by addition of 5 mM succinate or 4 mM pyruvate + 1 mM malonate and the increase in fluorescence was followed at excitation and emission wavelengths of 560 and 590 nm, respectively. Appropriate correction for background signals and standard curves generated using known amounts of H_2O_2 were used to calculate the rate of H_2O_2 production in nmol/min/mg mitochondrial protein. The percentage free radical leak, which is a measure of the number of electrons that produce superoxide (and subsequently H_2O_2) compared with the total number of electrons which pass thorough the respiratory chain, was calculated as the rate of H_2O_2 production divided by the rate of O_2 consumption (Barja et al., 1994).

Statistics

Values are presented as means ± SEM except Fig. 2D, in which error bars indicate SD. The significance of differences between means was assessed by the unpaired Student's *t*-test using Microsoft Excel; *P* values < 0.05 were taken to be significant.

Results

Cell growth and mitochondrial morphology

In general, cultured cells gain their energy mostly from glycolysis. Therefore, cells deficient in respiratory function can grow in normal medium, although possibly at a slower rate, relying predominantly on glycolysis (Hofhaus et al., 1996). Actually, ρ^0 cells, which lack mitochondrial DNA completely, can grow producing energy exclusively through glycolysis (King and Attardi, 1989). On the other hand, galactose metabolism via glycolysis is much slower than glucose metabolism (Reitzer et al., 1979). Therefore, cells in galactose medium are forced to oxidize pyruvate through the mitochondrial respiratory chain for energy required for growth. Consequently, cells with defects in their mitochondrial respiratory chains show growth impairments in galactose medium. To evaluate this phenomenon is also observed in our cells, we examined growth retardation by addition of mitochondrial complex I inhibitor, rotenone (Fig. 1A). In glucose medium, 10 nM rotenone had only a slight effect on the growth of PINK1$^{+/+}$ MEFs and slower growth was observed even in the presence of 100 nM rotenone. However, in the galactose medium, 10 nM rotenone significantly inhibited the growth of PINK1$^{+/+}$ MEFs and 100 nM roteone completely arrested the growth. Therefore, we could confirm that the growth impairment of our cells in the galactose medium was due to mitochondrial respiratory chain defects.

PINK1 acts upstream of parkin, regulating mitochondrial integrity and function; therefore, loss of PINK1 is considered to affect mitochondrial functions. To assess the mitochondrial functions of PINK1$^{-/-}$ MEFs, growth capability in a medium in which galactose replaced glucose was examined. As shown in Fig. 1B, PINK1$^{-/-}$ MEFs appeared to show clear growth impairments in the galactose medium, whereas PINK1$^{+/+}$ MEFs grew slightly slower than in the glucose medium.

No differences of mitochondrial morphology between PINK1$^{+/+}$ and $^{-/-}$ MEFs in the glucose medium were detected (Fig. 1C), consistent with the previous report (Matsuda et al., 2010). However, in the galactose medium, mitochondria of the PINK1$^{-/-}$ MEFs were more fragmented compared to the PINK$^{+/+}$ MEFs (Fig. 1C). This is consistent with previous reports, which found mitochondrial morphological changes were more pronounced when PINK1 knock-down HeLa cells were grown in low-glucose medium (Exner et al., 2007) and human PINK1 homozygous mutant fibroblast in galactose medium (Grünewald et al., 2009). In these cells, mitochondrial morphological changes were associated with the mitochondrial functional impairment.

Assessments of mitochondrial functions at the cellular level

Because PINK1$^{-/-}$ MEFs showed severe growth impairments in the galactose medium, the mitochondrial functions of these cells were assessed at the cellular level. First, cellular respiration rates were measured (Fig. 2A). The basal respiration rate was significantly reduced in PINK1$^{-/-}$ cells compared with that in PINK1$^{+/+}$ cells (11.13 ± 0.71 versus 14.36 ± 1.01 nmol O/min/10^6 cells; $p<0.05$; $n=5$ independent experiments), consistent with previous reports using partial knock-down of PINK1 expression (Gandhi et al., 2009; Liu et al., 2009). Oligomycin inhibits ATP synthase, resulting in non-phosphorylating respiration. FCCP uncouples oxidative phosphorylation, leading to maximum respiration rates. In both conditions, the

Please cite this article as: Amo, T., et al., Mitochondrial membrane potential decrease caused by loss of PINK1 is not due to proton leak, but to respiratory chain defects, Neurobiol. Dis. (2010), doi:10.1016/j.nbd.2010.08.027

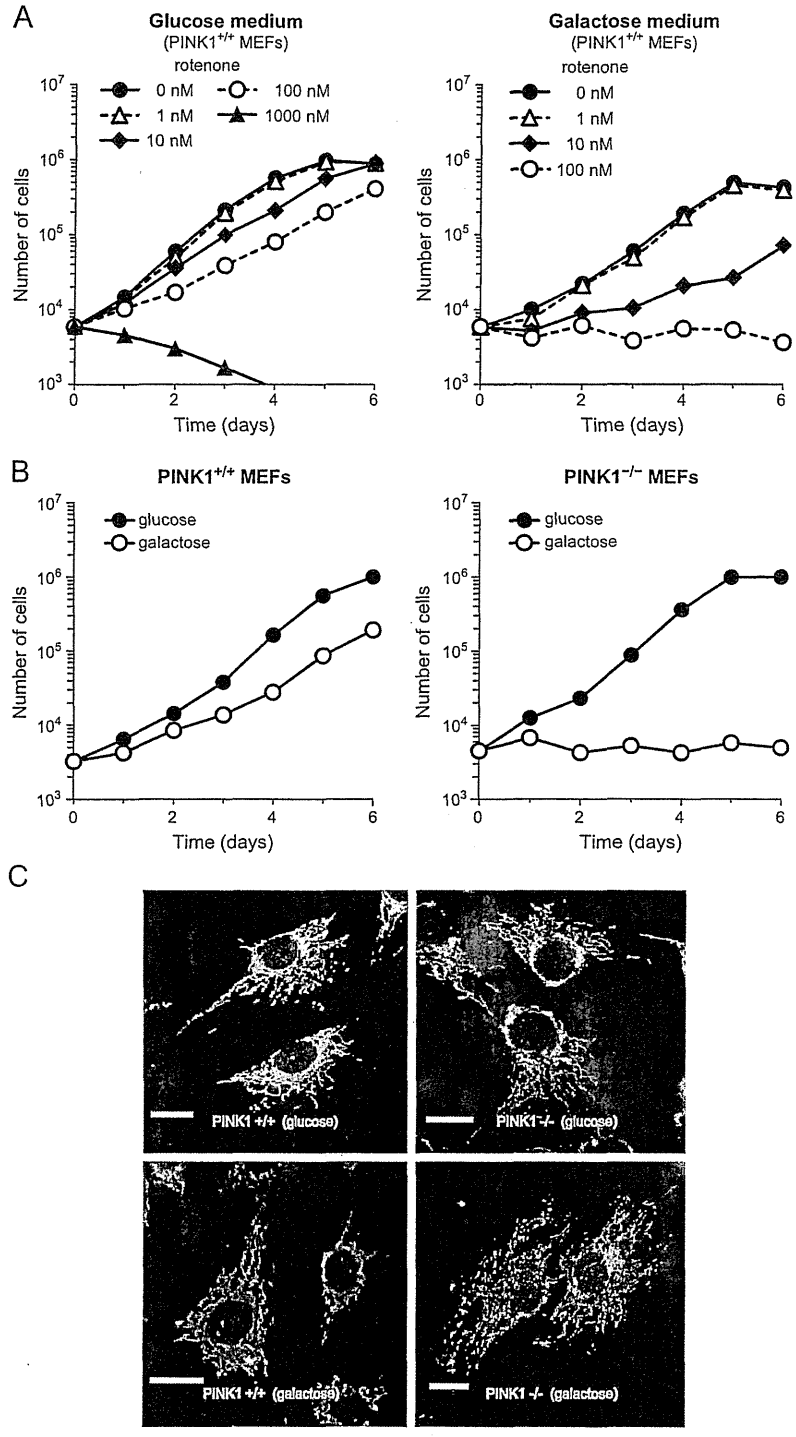

Fig. 1. (A) Growth retardation of PINK1$^{+/+}$ MEFs by mitochondrial complex I inhibitor, rotenone in glucose or galactose medium. Closed circles with solid line, 0 nM rotenone; open triangles with dashed line, 1 nM rotenone; closed diamonds with solid line, 10 nM rotenone; open circles with dashed line, 100 nM rotenone; closed triangles with solid line, 1000 nM rotenone. Cells grown in 12-well plates were trypsinized and live cells were assessed by trypan blue dye exclusion. (B) Growth curves of PINK1$^{+/+}$ and $^{-/-}$ MEFs. Closed symbols (*glucose*), growth curve for cells grown in DMEM containing 4.5 g/l glucose and 1 mM sodium pyruvate; open symbols (*galactose*), growth curve for cells grown in DMEM lacking glucose and containing instead 1.0 g/l galactose and 1 mM sodium pyruvate. Cells grown in 12-well plates were trypsinized and live cells were assessed by trypan blue dye exclusion. (C) Mitochondrial morphology of PINK1$^{+/+}$ and $^{-/-}$ MEFs. After incubating cells with the glucose or galactose medium for 24 hours, cells were fixed and immunostained with anti-Tom20 antibody to visualize mitochondria. Scale bar, 20 μm.

PINK1$^{-/-}$ cells respired significantly slower than the PINK1$^{+/+}$ cells (1.76 ± 0.13 versus 2.95 ± 0.27 ($p<0.01$; $n=5$ independent experiments) and 16.44 ± 1.80 versus 23.50 ± 1.18 nmol O/min/10^6 cells ($p<0.05$; $n=5$ independent experiments), respectively).

The main function of mitochondria is ATP synthesis via oxidative phosphorylation. ATP levels under basal conditions were significantly reduced in PINK1$^{-/-}$ MEFs (Fig. 2B), as reported previously for dissociated PINK1$^{-/-}$ mouse neurons (Gispert et al., 2009) and PINK1

Please cite this article as: Amo, T., et al., Mitochondrial membrane potential decrease caused by loss of PINK1 is not due to proton leak, but to respiratory chain defects, Neurobiol. Dis. (2010), doi:10.1016/j.nbd.2010.08.027

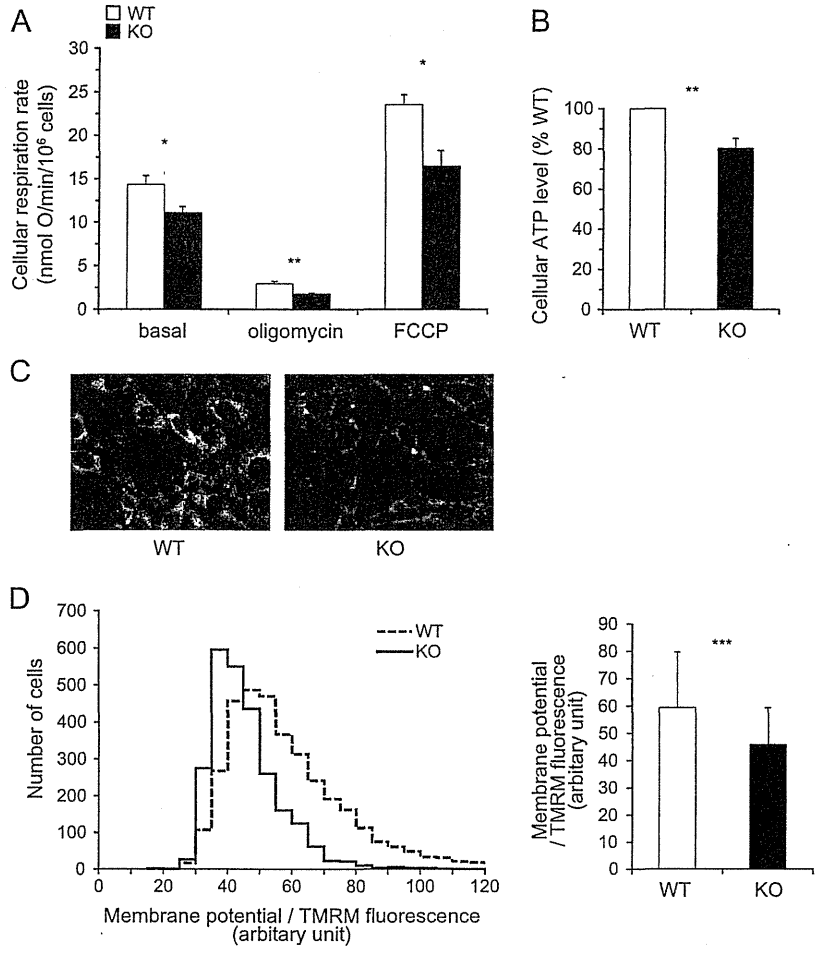

Fig. 2. Mitochondrial functions assessed at the cellular level. Open bars, PINK1$^{+/+}$ MEFs; closed bars, PINK1$^{-/-}$ MEFs. (A) Cell respiration rate of PINK1$^{+/+}$ and $^{-/-}$ MEFs. The oxygen respiration rate was measured at density of 8.0×10^6 cells/ml under each of the following three conditions: basal rate (no additions); State 4 (no ATP synthesis) [after addition of 1 μg/ml oligomycin], uncoupled [after addition of 3 μM FCCP]. After sequential measurements, the endogenous respiration rate was determined by adding 1 μM rotenone +2 μM myxothiazol. Error bars indicate SEM ($n=5$ independent experiments). (B) Cellular ATP levels. Data were normalized based on cell numbers and expressed as the percentage of the level in PINK1$^{+/+}$ cells. Error bars indicate SEM ($n=4$ independent experiments). (C) Live cell images of PINK1$^{+/+}$ and $^{-/-}$ MEFs with TMRM fluorescence. (D) Mitochondrial membrane potential evaluated by live cell imaging of TMRM fluorescence. *Left panel*, the distribution of TMRM fluorescence from 3537 PIINK1$^{+/+}$ and 2566 PINK1$^{-/-}$ cells from 12 wells per cell type; *right panel*, the average value of TMRM fluorescence per cell. Error bars indicate SD. *$P<0.05$; **$P<0.01$; ***$P<0.001$.

siRNA knock-down PC12 cells (Liu et al., 2009). Mitochondrial membrane potential was also measured by live cell imaging of TMRM fluorescence. Typical images were shown in Fig. 2C. The histogram shows the distribution of TMRM fluorescence from 3537 PINK1$^{+/+}$ cells and 2566 PINK1$^{-/-}$ cells from 12 wells per cell type and the bar graph indicates the mean ± SD of TMRM fluorescence per cell (Fig. 2D). According to the Nernst equation, the ratio of TMRM fluorescence would translate into, on average, 6.88 mV lower mitochondrial membrane potential in the PINK1$^{-/-}$ cells if the plasma membrane potentials were not different between PINK1$^{+/+}$ and $^{-/-}$ cells. Mitochondrial membrane potential decrease was also showed previously in PINK1 knock-down HeLa cells (Exner et al., 2007) and in stable PINK1 knock-down neuroblastoma cell lines (Sandebring et al., 2009).

Assessments of mitochondrial functions using isolated mitochondria

To further analyze mitochondrial functions, we measured the kinetics of oxidative phosphorylation using isolated mitochondria from PINK1$^{+/+}$ and $^{-/-}$ MEFs. Fig. 3 shows the kinetics of the three modules of oxidative phosphorylation using succinate as a respiratory substrate (complex II-linked respiration). Fig. 3A shows the kinetic response of substrate oxidation to its product, $\Delta\psi$. The substrate oxidation kinetic curve for PINK1$^{-/-}$ cells was clearly shifted lower compared with that for PINK1$^{+/+}$ cells, indicating that the loss of PINK1 caused mitochondrial respiratory chain defects. Fig. 3B shows the kinetic response of proton leak to its driving force, $\Delta\psi$, and Fig. 3C shows the kinetic response of the ATP phosphorylating pathway to its driving force, $\Delta\psi$. Both kinetic curves for PINK1$^{+/+}$ and $^{-/-}$ MEFs (open and closed symbols, respectively) were overlapping, implying that there were no significant differences in those modules.

We also independently measured the mitochondrial oxygen consumption rate using pyruvate/malate as a respiratory substrate instead of succinate to check complex I. Modular kinetic analysis using pyruvate/malate is technically difficult for the following reasons: (1) the oxygen consumption rate with pyruvate/malate is much slower than succinate respiration; and (2) there are no competitive inhibitors of complex I-linked respiration, such as malonate for succinate respiration. As shown in Fig. 4A, the respiration rates in State 3 and 4 with pyruvate/malate of isolated mitochondria from PINK1$^{-/-}$ cells (closed symbols) were significantly slower than those of PINK1$^{+/+}$ cells (open symbols), as in the case of succinate respiration (Fig. 4B; data derived from the kinetic curves in Fig. 3).

Please cite this article as: Amo, T., et al., Mitochondrial membrane potential decrease caused by loss of PINK1 is not due to proton leak, but to respiratory chain defects, Neurobiol. Dis. (2010), doi:10.1016/j.nbd.2010.08.027

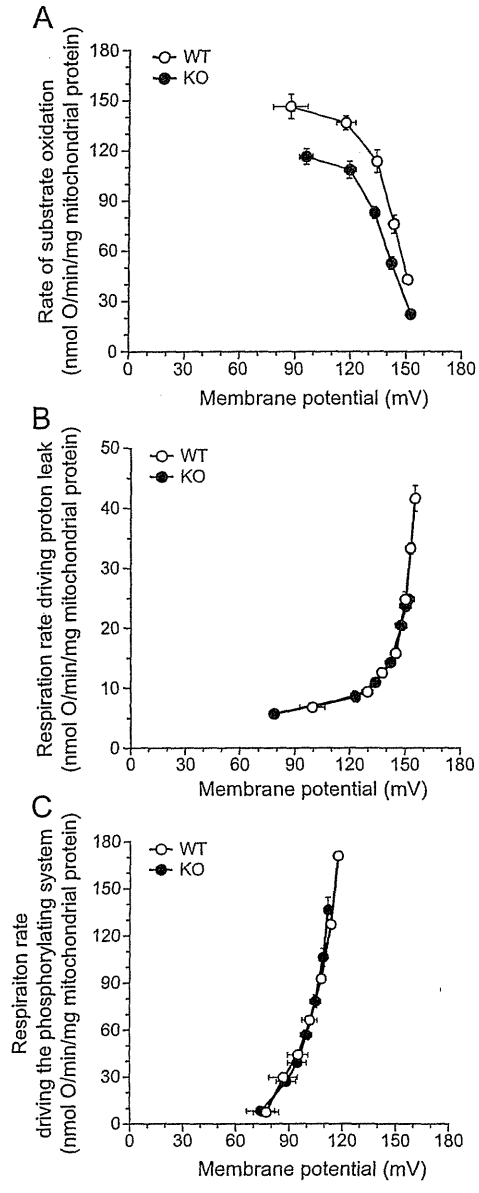

Fig. 3. Modular kinetic analysis of oxidative phosphorylation in mitochondria isolated from PINK1$^{+/+}$ and $^{-/-}$ MEFs. Modular kinetic analysis of the kinetic responses to membrane potential, $\Delta\psi$, of respiration driving (A) substrate oxidation ($\Delta\psi$ titrated with uncoupler, FCCP, starting in State 4), (B) proton leak ($\Delta\psi$ titrated with malonate, starting in State 4) and (C) the phosphorylating system, calculated by subtracting respiration driving proton leak from respiration driving the $\Delta\psi$-consumers ($\Delta\psi$ titrated with malonate starting in State 3; not shown) at each $\Delta\psi$. Open symbols, PINK1$^{+/+}$ MEFs; closed symbols, PINK1$^{-/-}$ MEFs. Error bars indicate SEM ($n=4$ independent mitochondrial preparations).

Mitochondrial ROS production

Mitochondrial ROS production rate was assessed by measurement of the H_2O_2 generation rate. Mechanisms of mitochondrial ROS production were well described elsewhere (Fig. 1 of Lambert et al., 2010). Pyruvate and malate generate NADH, which induced forward electron transport and generate ROS mainly from complex I and III. For pyruvate/malate respiration, the basal H_2O_2 generation rate (measured in the absence of respiratory chain inhibitors) was not different between PINK1$^{+/+}$ and $^{-/-}$ mitochondria (Fig. 4C). The addition of antimycin A and further addition of rotenone, which inhibited forward electron transport at complex III and I, respectively, enhanced H_2O_2 generation. During succinate respiration in the absence of respiratory chain inhibitors, ROS are generated mainly from the quinine binding site of complex I due to reverse electron flow from coenzyme Q to complex I. For succinate respiration, H_2O_2 generation rate in the absence of reparatory chain inhibitors was higher in PINK1$^{+/+}$ mitochondria than in PINK1$^{-/-}$ mitochondria, but the difference was not significant (Fig. 4D). The addition of rotenone, which blocks reverse electron flow from coenzyme Q to complex I, attenuated H_2O_2 generation.

Figs. 4 C and D show a tendency for PINK1$^{+/+}$ mitochondria to generate more ROS than PINK1$^{-/-}$ mitochondria. However, their respiration rates were remarkably different (Figs. 4A and B). Therefore, we calculated the percentage free radical leak, which is the fraction of molecules of O_2 consumed that give rise to H_2O_2 release by mitochondria (free radical leak) during either pyruvate/malate or succinate State 4 respiration (Figs. 4E and F). For pyruvate/malate respiration, mitochondria isolated from PINK1$^{-/-}$ cells had higher proportion of H_2O_2 generation than PINK1$^{+/+}$ mitochondria. During succinate respiration without respiratory inhibitors, PINK1$^{-/-}$ mitochondria had also higher proportion of free radical leak mainly from complex I due to reverse electron flow from coenzyme Q to complex I. Because the differences disappeared with addition of rotenone, which inhibit reverse electron flow, ROS generation enhanced by loss of PINK1 was mostly from complex I.

Discussion

We produced an *in vitro* model of Parkinson's disease, immortalized PINK1$^{-/-}$ MEFs. Previously, impairment of mitochondrial respiration was observed in the brains of PINK1$^{-/-}$ mice (Gautier et al., 2008). PINK1$^{-/-}$ MEFs clearly showed a phenotype of mitochondrial dysfunctions, which is consistent with PD pathogenesis. This phenotype was apparent in a cell growth experiment using medium containing galactose instead of glucose (Fig. 1B). Mitochondrial fragmentation was observed when PINK1$^{-/-}$ MEFs grew in the galactose medium (Fig. 1C), which was consistent with previous reports (Exner et al., 2007; Grünewald et al., 2009). Our results have unveiled that the PINK1$^{-/-}$ MEF line could be a potential PD model, presenting growth retardation due to decreased mitochondrial respiration activity. Thus, the PINK1$^{-/-}$ MEFs are a useful tool for evaluating the role of PINK1 in mitochondrial dysfunction and relevant to PD.

In PINK1$^{-/-}$ MEFs, mitochondrial membrane potential was decreased compared with that in littermate wild-type MEFs (Figs. 2C and D), as reported previously for PINK1 knock-down HeLa cells (Exner et al., 2007) and stable PINK1 knock-down neuroblastoma cell lines (Sandebring et al., 2009). This is a key event during elimination of mitochondria. Mitochondrial fission followed by selective fusion segregates damaged mitochondria, which decreases their membrane potential, and permits their removal by autophagy (Twig et al., 2008). The PINK1–parkin pathway is thought to have a crucial role in this mitochondrial elimination mechanism (Geisler et al., 2010; Kawajiri et al., 2010; Matsuda et al., 2010; Narendra et al., 2008, 2010; Vives-Bauza et al., 2010). To clarify what caused the decrease in mitochondrial membrane potential, we performed a modular kinetic analysis using isolated mitochondria (Fig. 3). This analyzes the kinetics of the whole of oxidative phosphorylation divided into three modules connected by their common substrate or product, mitochondrial membrane potential ($\Delta\psi$). The modules are include one $\Delta\psi$-producer (substrate oxidation) and two $\Delta\psi$-consumers (phosphorylating system and proton leak) (Brand, 1990). To decrease $\Delta\psi$, the $\Delta\psi$-producer should be down-regulated and/or $\Delta\psi$-consumers should be up-regulated. As cellular ATP levels were decreased compared with those in littermate wild-type MEFs (Fig. 2B), it is unlikely that the phosphorylating system is up-regulated. Indeed, the kinetics of the phosphorylation module were not altered (Fig. 3C). The other $\Delta\psi$-consumer, proton leak,

Please cite this article as: Amo, T., et al., Mitochondrial membrane potential decrease caused by loss of PINK1 is not due to proton leak, but to respiratory chain defects, Neurobiol. Dis. (2010), doi:10.1016/j.nbd.2010.08.027

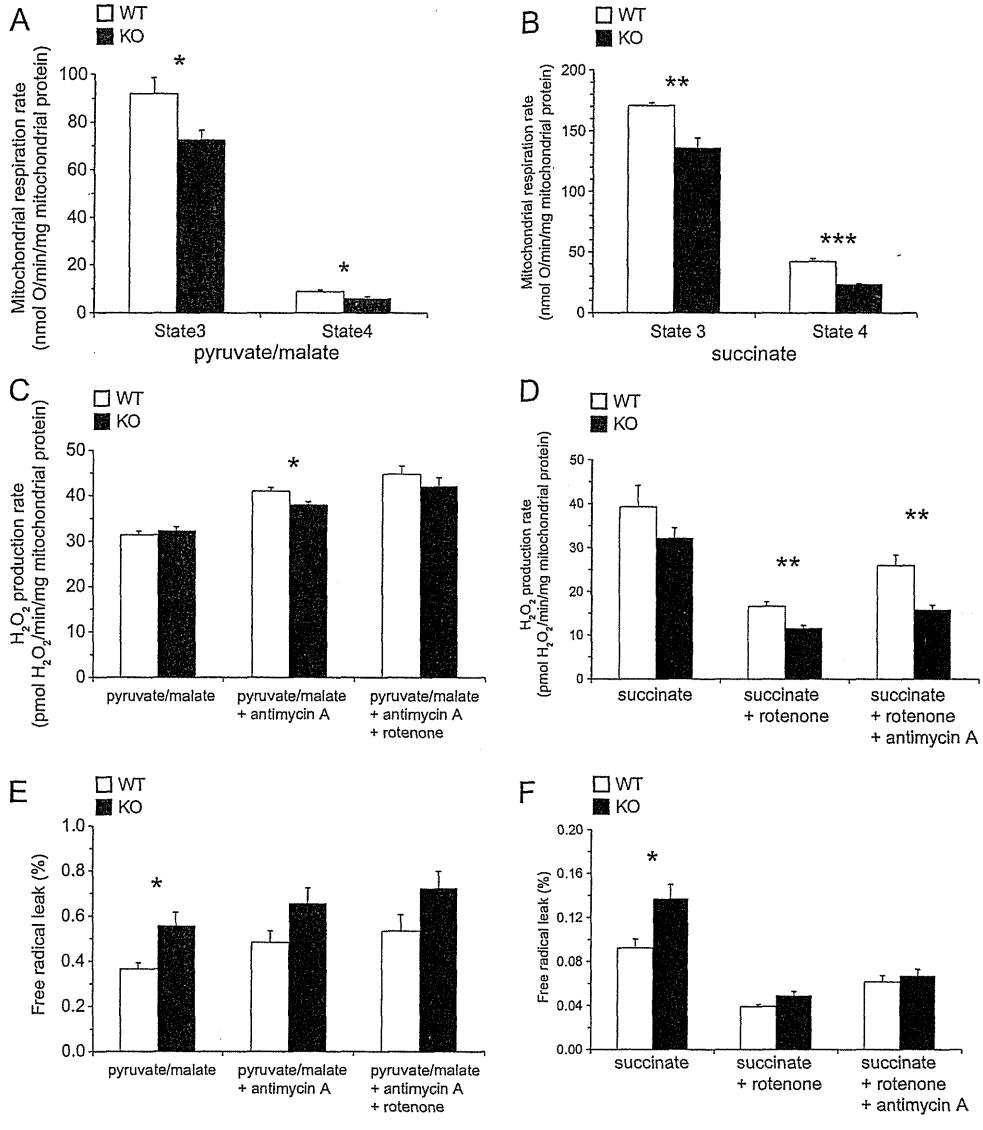

Fig. 4. Oxygen consumption rate and H_2O_2 production rate of mitochondria isolated from PINK1$^{+/+}$ and $^{-/-}$ MEFs. Open bars, PINK1$^{+/+}$ MEFs; closed bars, PINK1$^{-/-}$ MEFs. (A) State 3 and State 4 respiration rate of mitochondria with pyruvate/malate as a respiratory substrate. (B) State 3 and State 4 respiration rate of mitochondria with succinate as a respiratory substrate. Data were derived from the results of modular kinetic analysis (Fig. 3). State 3 respiration rates were the kinetic start points of the $\Delta\psi$-consumers (the sum of the phosphorylating system and proton leak). State 4 respiration rates were average values of the respiration rates at the kinetic start points of substrate oxidation and proton leak. (C, D) Mitochondrial H_2O_2 production rate with pyruvate/malate (C) or succinate (D) as a respiratory substrate. (E, F) Percentage free radical leak (FRL) for State 4 respiration with pyruvate/malate (E) or succinate (F) as a respiratory substrate. Error bars indicate SEM ($n=5$ and 4 independent mitochondrial preparations for pyruvate/malate and succinate respiration, respectively). *$P<0.05$; **$P<0.01$; ***$P<0.001$.

which partially dissipates the membrane potential without ATP synthesis, was also not changed (Fig. 3B). Therefore, the decrease in membrane potential caused by loss of PINK1 is likely to have been caused only by lower activity of the $\Delta\psi$-producer, substrate oxidation (Fig. 3A). This is the first report showing that mitochondrial membrane potential decrease caused by loss of PINK1, which is the key event for the following mitochondrial elimination, was not due to proton leak, but to respiratory chain defects. We used only succinate (a complex II-linked substrate) as a respiratory substrate in the modular kinetic analysis for technical reasons. However, complex I-linked respiration (pyruvate/malate) was also decreased in PINK1$^{-/-}$ MEFs like succinate respiration (Fig. 4A).

The mitochondrial respiration rates in State 4 were decreased in PINK1$^{-/-}$ MEFs, and consequently, the proportions of free radical leak were significantly higher in PINK1$^{-/-}$ MEFs than in PINK1$^{+/+}$ MEFs (Figs. 4E and F). Because the differences disappeared with addition of rotenone (complex I inhibitor, which inhibits reverse electron flow from coenzyme Q to complex I), ROS generation enhanced by loss of PINK1 was mostly from complex I. These results are partially consistent with those in previous reports, suggesting that MPTP and rotenone induce neuronal cell death by inhibiting complex I activity, leading to a PD-like phenotype (Dauer and Przedborski, 2003; Jackson-Lewis and Przedborski, 2007; Trojanowski, 2003).

In this study, we developed an *in vitro* PD model, the PINK1$^{-/-}$ MEF line, and established the experimental conditions for cell growth to detect mitochondrial dysfunction. This is the first report showing that complete ablation of PINK1 causes a decrease in mitochondrial membrane potential, which is not due to proton leak, but to respiratory chain defects.

Please cite this article as: Amo, T., et al., Mitochondrial membrane potential decrease caused by loss of PINK1 is not due to proton leak, but to respiratory chain defects, Neurobiol. Dis. (2010), doi:10.1016/j.nbd.2010.08.027